reproduced. The parameter E required to provide the best fit is indicative of a root-mean-square surface diffusion distance for these molecules in the tens of microns range. The SiO effusion from graphite cells[6] on the other hand deviates from the properties predicted with a model that assumes the adsorbed species do not interact. Indications are that a model attributing a repulsive interaction between the adsorbed molecules would yield predictions more nearly in agreement with the experimental results.

Results[14] which show directly that the spatial distribution is dependent upon the molecular species itself provide additional evidence to support the effusion model being tested. The effusion distributions for the monomer and dimer of potassium chloride are only qualitatively consistent with the behavior predicted by the coupled vapor–surface transport model.

Over all, the results of the comparison suggest that the coupled surface- and vapor-transport model[2] can bring a semblance of coherency into a field that has been fraught with anomalous results for many years. For some vapor–solid systems, the assumption of noninteracting adsorbed species may have to be removed to improve the general applicability of the theory.[15] With the adoption of a suitable model for the effusion process, however, the accuracy and applicability of an already valuable tool will be greatly enhanced.

ACKNOWLEDGMENTS

The author is indebted to Dr. N. A. Gjostein for his review of the manuscript. The interest and critical comments of Professor J. P. Hirth and T. Dunham concerning this work are also gratefully acknowledged.

[15] W. L. Winterbottom (unpublished).

THE JOURNAL OF CHEMICAL PHYSICS VOLUME 49, NUMBER 1 1 JULY 1968

Rydberg States and Scattering States of Molecular Electrons: e–H_2^+

R. STEPHEN BERRY

Department of Chemistry and The James Franck Institute, University of Chicago, Chicago, Illinois

AND

SVEND ERIK NIELSEN

Chemistry Laboratory III, H. C. Ørsted Institute, University of Copenhagen, Copenhagen, Denmark

(Received 29 January 1968)

A general method is presented for obtaining a model potential for calculation of Rydberg states and ionized states of an electron in a diatomic (or more complex) molecule. The potential is derived from a known wavefunction for the ionic molecule core by expanding the charge distribution, including the fixed-position nuclei, in spherical harmonics. Exchange effects are included in the form of an effective local $\rho^{1/3}$ potential. The method is applied to the Rydberg states of H_2 to examine the various contributions to the level splittings and the dependence of these on internuclear distance R. It is also applied to the determination of phase shifts in e–H_2^+ scattering and to the dependence of these phase shifts on R. The particular utility of the method is the ease and efficiency with which one can explore the behavior of electronic contributions to a wide variety of matrix elements, as functions of all the parameters n(or E), l, m, and R.

I. INTRODUCTION

Many low-energy electron–molecule processes appear to require for their elucidation, reasonably thorough knowledge of highly excited molecular Rydberg states and of the corresponding low-energy scattering states, as functions of internuclear distances. Such processes encompass an entire class of vibronically induced phenomena: autoionization, associative ionization and dissociative recombination, Penning ionization, some collisional excitation processes, and vibronic perturbations of bound Rydberg states, among others. In order to study these processes in a systematic way, we have first investigated the behavior of the scattering states of an electron in the field of H_2^+ molecule–ion and of the corresponding molecular Rydberg states. In the work reported here, we have done this in a manner designed to be efficient for studying dependence on the various parameters such as energy, internuclear distance, and angular momentum, and not, at this stage, for ultimate accuracy. Specifically, we have constructed a reasonably realistic model potential for H_2^+ and computed from it bound Rydberg-state energies and wavefunctions, and continuum phase shifts and wavefunctions. From these calculations, we draw several direct inferences about the behavior of energies and quantum defects of Rydberg states and of continuum phase shifts.

In the discussion that follows, we first describe the model and the method of calculation. Next, we describe

the Rydberg states and present our conclusions about them, and finally, we discuss the continuum states and phase shifts.

II. THE MODEL

Our H_2^+ potential is a truncated form of an expansion of the molecular-core Hamiltonian in spherical harmonics. One can write such an expansion in as accurate or approximate form as one chooses; one may use something as crude as a point-multipole representation,[1] or as sophisticated as a Hartree–Fock potential, as Wilkins and Taylor have recently done.[2] We have chosen something between these two extremes. Specifically, we define our zero-order Hamiltonian

$$\mathcal{H}_0 = -\tfrac{1}{2}\nabla^2 + V_{0c} + V_{0E} \tag{1}$$

and a first-order correction,

$$\mathcal{H}_1 = V_{2c}, \tag{2}$$

where the potentials V_{0c} and V_{0E} are the Coulomb and exchange parts of the spherically symmetric potential and V_{2c} is the Coulomb part of the potential depending on $P_2(\cos\theta)$. The potentials are based on the wavefunctions $\psi(H_2^+; R; \mathbf{r})$, of H_2^+ obtained by Bates, Ledsham, and Stewart[3] in the Born–Oppenheimer approximation. The Coulomb term V_{0c} has the form

$$V_{0c}(r, R) = r^{-1}\int_0^r \rho(s)s^2 ds + \int_r^\infty \rho(s)s\,ds - 2/r, \quad r > R/2$$
$$-4/R, \quad r < R/2$$

where

$$\rho(s) = \int_0^\pi \sin\theta d\theta \int_0^{2\pi} d\phi \,|\, \psi(\mathrm{H_2^+}; R; s; \theta; \phi) \,|^2. \tag{3}$$

Thus V_{0c} corresponds to the spherical average of the entire charge density, including the nuclei. Note that V_{0c} corresponds to a penetrable charge distribution, and not a point monopole. For efficiency, it was desirable to use a local approximation to the actual nonlocal exchange potential. We chose the method of Slater,[4] as modified by Tong and Sham,[5] in which the exchange potential depends on ρ, the charge density, as $\rho^{1/3}$:

$$V_{0E}(r) = -[3\rho(r)/\pi]^{1/3}. \tag{4}$$

Examples of the potentials $V_{0c}+V_{0E}$ (or V_{0cE}) are shown in Fig. 1. The Schrödinger equations

$$\mathcal{H}_0\psi_{nl}^0 = \epsilon_{nl}^0\psi_{nl} \tag{5}$$

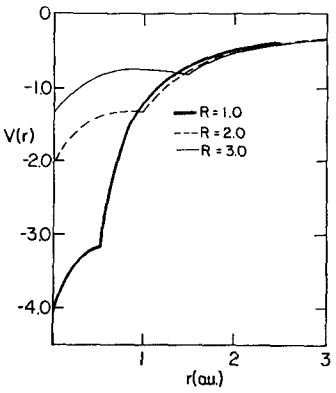

FIG. 1. Spherical potentials $V_{0cE}(r, R)$. R values are in a.u.

and

$$\mathcal{H}_0\psi_{kl}^0 = (k^2/2)\psi_{kl}^0 \tag{6}$$

were solved numerically by Numerov integration. For the scattering states, the functions ψ_{kl}^0 were used directly to obtain phase shifts. For the bound states, we were interested both in the levels in $V_{0c}+V_{0E}$ and in the amount of l spoiling due to the nonspherical part of the core; we used the quadrupolar Coulomb part V_{2c} as a perturbation to couple states of different l (as well as states of different n and the same l):

$$V_{2c}(r, R) = \tfrac{1}{2}(3\cos^2\theta - 1)$$
$$\times\left[\frac{1}{r^3}\int_0^r \rho_2(s)s^4 ds + r^2\int_r^\infty \rho_2(s)s^{-1}ds\right],$$

where

$$\rho_2(s) = \int_0^\pi \sin\theta_1 d\theta_1 \int_0^{2\pi} \tfrac{1}{2}(3\cos^2\theta_1 - 1)\,d\phi_1$$
$$\times \,|\, \psi(\mathrm{H_2^+}; R; s; \theta_1; \phi_1) \,|^2. \tag{7}$$

The matrices of $V_{2c}(R)$ were diagonalized in various truncated forms described below, to give functions $\psi^{(1)}$ which, as it turns out, can still be usefully classified by the subscripts n and l.

Thus our continuum functions ψ_{kl}^0 and the zero-order bound-state functions ψ_{nl}^0 are eigenfunctions of l as well as of l_z, while the slightly more refined functions $\psi_{nl}^{(1)}$ are, at best, approximate eigenfunctions of l but, because of cylindrical symmetry, are eigenfunctions of l_z.

The bound zero-order functions ψ_{nl}^0 and eigenvalues ϵ_{nl}^0 were obtained with a search program based on outward integration only. The criterion of choice for each eigenvalue and eigenfunction was simply this. The best function was that one which extended to the largest distance r in the outer classically forbidden region before it began to diverge away from the axis of $\psi(r) = 0$. The energy step size was 10^{-4} a.u. (near convergence; larger steps were used to get first approximations). The basic step size in r was 0.025 a.u., and was checked by redoing some of the integrations with steps of 0.01

[1] See, for example, R. S. Berry, J. Chem. Phys. **45**, 1228 (1966). [Note, with reference to this paper, J. N. Bardsley, Chem. Phys. Letters **1**, 229 (1967)].
[2] R. L. Wilkins and H. S. Taylor, J. Chem. Phys. **47**, 3532 (1967).
[3] D. R. Bates, K. Ledsham, and A. L. Stewart, Phil. Trans. Roy. Soc. (London) **A246**, 215 (1953).
[4] J. C. Slater, Phys. Rev. **81**, 385 (1951).
[5] B. Y. Tong and L. T. Sham, Phys. Rev. **144**, 1 (1966).

TABLE I. Term values of Rydberg states in the potential V_{0cE}. (R and term values are in atomic units.)

l	n	$R=1.0$	$R=2.0$	$R=3.0$	$R=4.0$
$l=0$	3	0.0988	0.0860	0.0763	0.0688
	4	0.0470	0.0428	0.0396	0.0366
	5	0.0275	0.0256	0.0241	0.0226
	6	0.0180	0.0170	0.0162	0.0154
$l=1$	3	0.0714	0.0691	0.0644	0.0592
	4	0.0374	0.0364	0.0347	0.0326
	5	0.0230	0.0225	0.0217	0.0206
	6	0.0156	0.0153	0.0148	0.0142
$l=2$	3	0.0578	0.0587	0.0584	0.0583
	4	0.0324	0.0328	0.0328	0.0324
	5	0.0206	0.0208	0.0208	0.0206
	6	0.0143	0.0143	0.0143	0.0142
$l=3$	4	0.0313	0.0313	0.0313	0.0314
	5	0.0200	0.0201	0.0201	0.0201
	6	0.0139	0.0139	0.0139	0.0139

bohr. A further check was obtained by comparing the quantum defects μ_{nl} obtained with the bound-state integration and those extrapolated from the short-range phase shifts of the low-energy continuum states, for if $2\pi k^{-1} \gg 1$ (k in a.u.),

$$\lim_{n\to\infty} \cot[\pi\mu_{nl}(R)] = \cot\eta_l(R).$$

The agreement was exact, within our accuracy; the phase shifts giving 3–4 significant figures for μ and the bound-state eigenvalues, 2.

Note that our potential makes no allowance for electron spin. In this sense the energies correspond to the averages of singlet and triplet Rydberg-state energies that one would find if the singlet–triplet splittings were due entirely to exchange integrals and not at all to differences in the Rydberg orbitals of corresponding singlets and triplets. This distinction between the sources of Rydberg singlet–triplet splittings was discussed by Mulliken.[6]

The continuum functions were also obtained with integration steps of 0.025 a.u. The short-range phase shifts are easily determined by the condition that outside the range of the short-range potential, if $\psi_{kl}^0(r_0)=0$,

$$\tan\eta_{kl} = -F_{kl}(kr_0)/G_{kl}(kr_0), \qquad (8)$$

where $F_{kl}(kr)$ and $G_{kl}(kr)$ are the conventional regular and irregular Coulomb functions as defined by Abramowitz.[7] For energies $\gtrsim 2\times10^{-2}$ a.u., the asymptotic sinelike and cosinelike forms can be used for $F_{kl}(r)$ and $G_{kl}(r)$. For lower energies, the evaluation of $F_{kl}(r)$ is accomplished easily in terms of the Bessel–Clifford functions[8]; the irregular function $G_{k0}(r)$ was evaluated by the same method, and for higher l values, by means of the recursion relation (cf. Ref. 7, Eqs. 14.2.3 and 14.2.4).

III. RESULTS: BOUND STATES

The zero-order bound-state energies ϵ_{nl}^0, are given in Table I, for various values of the internuclear distance R. Our approximate exchange potential corresponds to the Rydberg electron with random spin with respect to the spin of the core electron. Hence the appropriate comparison between our term values and the experimental, for example, is with the statistically weighted average, $\frac{1}{4}[E(\text{singlet})+3E(\text{triplet})]$, for each nlm_l configuration.

Table II contains the bound state energies ϵ_{nlm} for $R=2.0$. These energies were obtained by diagonalizing the matrix $(\psi_{nlm}^0 \mid V_{0cE}+V_{2c} \mid \psi_{n'l'm}^0)$, so that the energies correspond physically to the levels of an electron in a spherically averaged H_2^+ Coulomb potential, plus the spherically averaged effective local-exchange potential, plus the electrostatic quadrupolar potential. Table II also includes the weighted averages of the energies computed by Hazi and Rice, from a pseudopotential method,[9] and in the few cases where both singlet and

TABLE II. Term values for Rydberg electron in H_2. The internuclear distance $R=2.0$ a.u. Columns "Hazi and Rice" and "Experimental" give averages of singlet and triplet energies. The $F(l=3)$ splittings are essentially zero (±0.001) and are omitted. Figures in the column marked "δ" are the quantum defects corresponding to the column "This work."

n	l	m_l	This work ($V_{0cE}+V_{2c}$)	δ	Hazi and Rice (Pseudopotential)	Experimental
3	0	0	0.0860	0.59		
4			0.0428	0.58		
5			0.0256	0.58		
6			0.0170	0.58		
3	1	0	0.0821	0.53	0.0726	0.0764
4			0.0397	0.45	0.0380	0.0381
5			0.0238	0.42	0.0233	
6			0.0160	0.40		
3	1	1	0.0639	0.20	0.0558	0.0570
4			0.0343	0.19	0.0313	0.0319
5			0.0214	0.17	0.0200	0.0205
6			0.0145	0.13		
3	2	0	0.0605	0.17		
4			0.0324	0.07		
5			0.0211	0.13		
6			0.0144	0.11		
3	2	1	0.0596	0.10		
4			0.0322	0.06		
5			0.0210	0.12		
6			0.0144	0.11		
3	2	2	0.0570	0.04		
4			0.0315	0.02		
5			0.0204	0.04		
6			0.0141	0.04		

[6] R. S. Mulliken, J. Am. Chem. Soc. **86**, 3188 (1964).

[7] M. Abramowitz and I. A. Stegun, *Handbook of Mathematical Functions, National Bureau of Standards Applied Mathematics Series, No. 55* (U. S. Government Printing Office, Washington, D.C., 1964.

[8] C. Fröberg, Rev. Mod. Phys. **27**, 399 (1955).

[9] A. U. Hazi and S. A. Rice, J. Chem. Phys. **47**, 1125 (1967).

triplet terms are known for the same n, l, and m, the weighted experimental average energies as well.

It was our original intent to develop the method described here as a useful and efficient model for studying the electronic factors of a variety of matrix elements. The fact that the energies listed as "This Work" in Table II are in rather good agreement with those derived from the work of Hazi and Rice, and with the available experimental results, gives us considerable reassurance of the realistic nature of the model. The agreement also gives us confidence to use our results to give physical interpretation to the factors determining the energies of Rydberg states.

In the framework of this interpretation, the first and most obvious inference pertains to the origin of singlet–triplet splittings of Rydberg states. The reasonably good agreement of the energies in Table II shows that the principal source of singlet–triplet splittings in Rydberg states is the exchange interaction between the Rydberg electron and the core electron, rather than the difference between the Rydberg orbital in the singlet and triplet states. This was suspected by Mulliken when he chose to focus attention on the quantum defects associated with the average energies and not on those of singlets and triplets separately. The dominance of the exchange contribution to the splitting clearly increases with principal quantum number. One can see this graphically in the column for $R=2.0$ a.u. in Fig. 2.

The second kind of inference we draw concerns the relative roles of the spherical and nonspherical contributions to the potential, and on the behavior of energies as functions of n, l, and m as the internuclear distance varies. Figure 2 gives a summary picture of these effects. As R increases, and the spherical well becomes shallower, the splitting of levels with the same n but different l decreases. If $R=1.0$ a.u., the separations between $E(n, l)$ and $E(n, l')$ is comparable to that between $E(n, l)$ and $E(n+1, l)$; if R is 3 a.u. or larger, the levels fall into well-defined groups according to the value of n. By contrast (and as one expects intuitively), the splitting due to the nonspherical potential V_{c2} increases very much, particularly as R increases from 1 to 2 a.u. By the time R is 3 or larger, the quadrupole effects overwhelm the nonhydrogenic spherical contributions, to the point that the $3p\sigma_u$ level lies below the $3s\sigma_g$, and the $3p\pi_u$ lies above the $3d\sigma_g$ and $3d\pi_g$.

The largest effects of the nonspherical potential are of course on the np levels, and the effects grow smaller as l increases, for a given n and R. The splittings and shifts of the various m states for $l=3$ are too small to show on the scale of Fig. 2 and have been omitted. It is reassuring that the model not only gives reasonably good agreement with experiment for $n\geq 4$, but that even for $n\geq 3$, the σ–π splittings are in good agreement with experiment. We can have confidence that using $V_{0cE}+V_{2c}$ to model the potential of H_2^+ will be a fairly reliable procedure.

Another kind of information we can extract is the

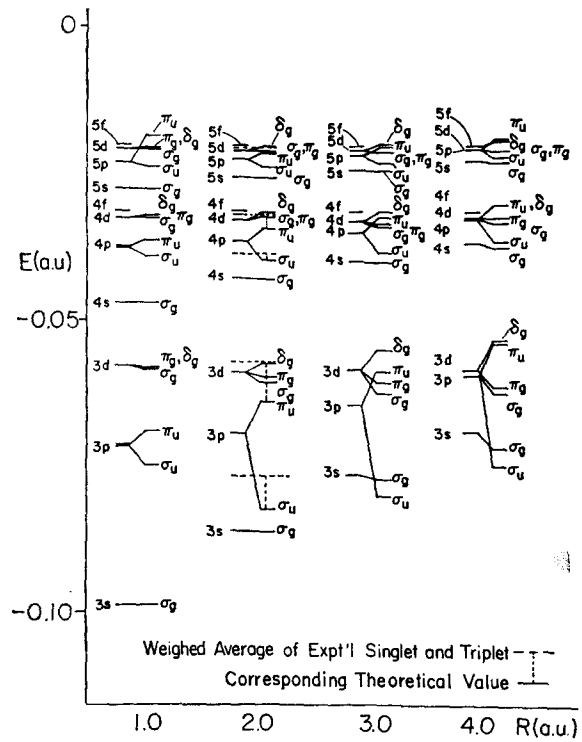

FIG. 2. Behavior of Rydberg term values in the spherical potential V_{0cE} and the nonspherical potential $V_{0cE}+V_{2c}$ for various values of R. Where experimental values are available, the statistically weighted average energy of singlet and triplet nlm levels are shown as dotted lines. Each of these is connected by a dotted line to the calculated level to which it corresponds. Splittings and shifts of f levels are omitted; they are all zero within the accuracy of our figures. The $n=6$ levels were the highest included in our computations and are omitted from this table because, without the $n=7$ levels in the calculation, the computed $n=6$ energies are definitely not reliable.

structure of the eigenvectors for the potential $V_{0cE}+V_{2c}$. Even for the most extreme case, the lowest $m_l=0$ orbital at $R=4.0$ a.u., the eigenvector is composed 72% of the lowest $m_l=0$ function in our set, the $3s$ function. The next basis function in importance to the lowest function is the $3d$, which contributes 25%. The next $m_l=0$ eigenfunction has essentially the same contributions in reverse order; it is 72% $3d$ and 26% $3s$. At $R=2.0$, essentially equilibrium distance, the $3s$ and $3d$ functions comprise 99% of the lowest and next-lowest $m_l=0$ eigenfunctions; even for $R=3.0$, the lowest functions are over 90% $3s$ and $3d$. In other words, the low-lying functions are only affected when R gets quite large, and when they are affected, the effect shows as a mixing of $\psi_{nl}{}^0$ and $\psi_{nl'}{}^0$. The functions of higher n are affected less in general, and in a somewhat different way. At $R=2.0$, all the functions with $n=4$, 5, or 6 are 99+% composed of their parent function; all the other basis functions enter with coefficients of about the same magnitude, $2\text{–}6\times 10^{-2}$. The effects of V_{2c} at $R=1.0$ are still smaller, and are only slightly larger at $R=3.0$. Thus the l spoiling by V_{2c} is a relatively small effect for $R\leq 3.0$; only for $R\sim 4.0$ does its effect become sig-

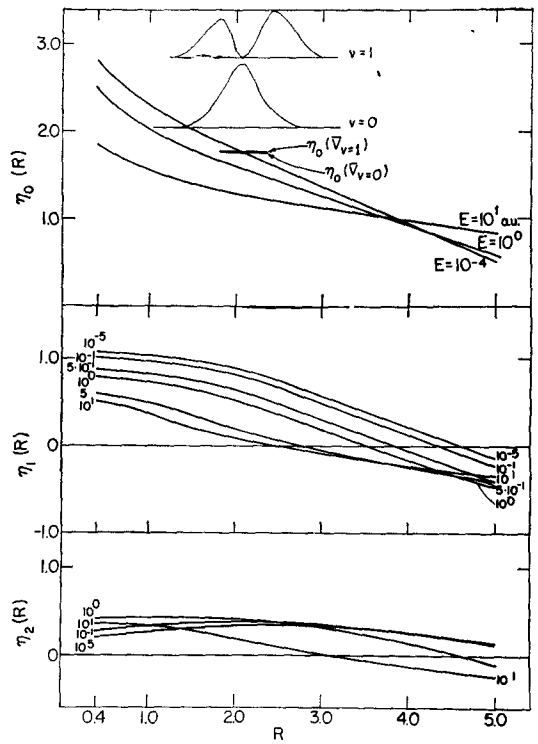

FIG. 3. Short-range phase shifts $\eta_l(R)$ for various energies, as functions of R. (a): $l=0$; (b): $l=1$; (c): $l=2$. The vibrational distribution functions for the two lowest states of H_2^+ are shown at the top, on the same horizontal scale as the phase shifts. The two parallel horizontal lines shown in (a) are the s-wave phase shifts obtained in potentials derived by averaging $V_{0cE}(R)$ over the vibrational distribution functions for $v=0$ and $v=1$. *Note added in proof*: Steepest curve for η_0 is for 10^{-5}, not 10^{-4} a.u.; curve for η_2 marked 10^5 is for 10^{-5} a.u., not 10^5 a.u.

nificant in the $n=3$ shell, and even there the orbital united atom parentage is still apparent.

It would be possible to extend the present method in various ways to obtain more refined values for bound-state energies. For example one could use the eigenfunctions obtained from the diagonalization just described, together with an accurate ground-state orbital, to obtain exchange integrals to estimate singlet–triplet splittings. Further, one could add higher terms to the potential: the higher Coulomb terms and the nonspherical contributions to the effective exchange. However in view of the accuracy of the pseudopotential method,[9] these extensions seem superfluous. Rather, a more fruitful direction appears to be one in which potentials of the type we have used are taken as the model potentials for a mixed perturbation–pseudopotential method, in which one combines the use of accurately known bound-state functions with a passing good model for the core potential to obtain scattering functions and highly excited bound-state functions.[10]

[10] B. Schneider, M. Weinberg, J. Tully, and R. S. Berry, "A Pseudopotential Method for Low-Energy Electron Scattering" (to be published).

IV. RESULTS: SCATTERING STATES

Our investigation of the scattering states is restricted to scattering by the spherical potential $V_{0cE}(R)$. We are particularly interested in two questions of general import for the problem of how best to handle electron–molecule scattering computations. The first is this: how does the scattering phase, or more specifically the short-range contribution η_l to the scattering phase depend on the internuclear distance? The second question, following the first, is: how does the R dependence of η_l depend on the electronic orbital angular momentum l? With this information, one can decide whether the electronic contribution, to an inelastic scattering amplitude for example, can be evaluated at only one internuclear distance and treated as a factorable constant, or whether one must go through the more lengthy evaluation of the electronic contribution at various values of R and then integrate this function together with the vibrational factor, over the appropriate range of R. If the phase η_l changes by a significant fraction of $\pi/2$ over the pertinent range of R, then one is forced to do the extended calculation; if the variation in η_l is much smaller than $\pi/2$ in the region of interest, then the electronic contribution can usually be treated reasonably as a constant.

The answers to our questions are given very explicitly by the curves shown in Fig. 3. The largest variation in $\eta_l(R, E)$ is of course that of η_0 for the lowest energies. Near the equilibrium distance of H_2^+, around $R=2$ a.u., this phase varies with R at a rate of approximately 0.4 rad/a.u. The classical amplitudes of the lowest vibrational states of H_2^+ are small, about 0.32 a.u. for $v=0$ and about 0.45 a.u. for $v=1$, for example. Consequently, when one is dealing with processes involving these states, one can justify evaluating the electronic contribution at $R=2$ and treating it as a constant. However for the $v=9$ state, the classical vibration amplitude of H_2^+ is approximately 1 a.u. Therefore η_0 varies over approximately 0.4 rad for this state, so that one is obliged in treating any process involving the states with $v \gtrsim 9$ of H_2^+, to treat the electronic contribution as a function of internuclear distance.

As a guide, one can use these generalizations: near $R=2$ bohr radii, and over the energy range from 10^{-5} to 10 a.u., the short-range part of the s-wave phase has an R derivative between -0.20 and -0.40 rad a.u.$^{-1}$; that of the p-wave shift lies between -0.18 and -0.3 rad a.u.$^{-1}$, and the d-wave variation with R lies between $+0.06$ and -0.20 rad a.u.$^{-1}$.

The curve of Fig. 4 exhibits the variation in $d\eta_l(R, E)/dR$ with energy. Insofar as the e–H_2^+ interaction can be taken as a guide for electron–molecule ion processes in general, one can estimate directly from Fig. 4 whether η_l will vary enough to warrant a "long-way" calculation. As one example, we can cite autoionization of H_2 (which goes largely into low-v states of H_2^+), as a case where one is justified in using the

simpler approximate procedure of finding electronic contributions at $R=R_e(H_2^+)$ only.[1] Examples of the other sort are associative ionization of H^*+H,[11] and the autoionization processes that couple with dissociative excitation of H_2.[12] In these cases, the transition amplitudes receive significant contributions from large enough ranges of R that one must be prepared to find large R dependences in the electronic factors of these amplitudes.

We also computed the phase shifts in two potential wells corresponding to a different physical situation, namely to a particle moving slowly with respect to the molecular vibration. This situation is the reverse of the Born–Oppenheimer problem and may arise in the case of scattering of very low-energy negative muons or of H^-. It is also instructive to see the difference between the phase shift for scattering by $V(R_e)$, the mean of the phase shifts taken over the vibrational distribution, and the phase shift due to the mean

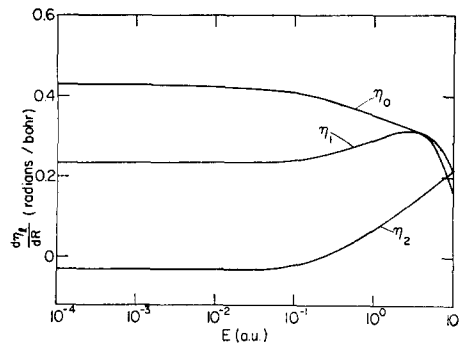

FIG. 4. The derivative $d\eta_l/dR \mid_{R=2.0}$ as a function of energy.

[11] Sv. E. Nielsen ad J. S. Dahler, J. Chem. Phys. **45**, 4060 (1966).
[12] G. H. Dunn and R. Van Zyl (private communication).

TABLE III. Typical S-wave phase shifts (radians) for various treatments of vibrational effects.

E (a.u.)	$\langle\eta_0(R)\rangle$ $v=0$	$\langle\eta_0(R)\rangle$ $v=1$	$\eta_0(2.0)$	$\eta_0(\bar{V}_v)$ $v=0$	$\eta_0(\bar{V}_v)$ $v=1$
10^{-2}	1.779	1.725	1.801	1.786	1.836
1	1.591	1.547	1.610	1.591	1.622

potentials, $\bar{V}_v$ determined by averaging $V_{0eE}(R)$ over the vth vibrational state of H_2^+. Typical values, shown in Table III, indicate how the three differ. From most problems, the average $\bar{\eta}$, taken over the appropriate R distribution, is the most nearly accurate. From the foregoing discussion, it is clear that $\eta(R_e)$ is a good approximation to $\bar{\eta}$ if only the first few vibrational states need be considered. The phase shifts based on $\bar{V}_0$ are essentially the same as $\bar{\eta}(v=0)$ and $\eta(R_e)$, but those based on $\bar{V}_1$ show significant positive deviations. This result indicates that the deviation from "Born–Oppenheimer" scattering may eventually be observable in comparisons of large angle e^-–H_2^+ scattering with μ^-–H_2^+ scattering at the same relative momentum. The figures for phase shifts for the $v=1$ state in Table III indicate that deviations as large as 0.1 rad may occur for momenta of 1 a.u. or less.

ACKNOWLEDGMENTS

This work was supported in part by the National Science Foundation, under Grant GP-5535. R. S. B. would like to express his gratitude for the hospitality of the H. C. Ørsted Institute, where much of the work was carried out. We would like to thank the NEUCC, Lyngby, Denmark, for the use of its computation facilities.